

1019

Dynamic Water, Fat, R_2^* and B_0 Field Inhomogeneity Quantification Using Multi-Echo Multi-Spoke Radial FLASH

Zhengguo Tan^{1,2}, Peter Dechent³, Xiaoqing Wang^{1,2}, Nick Scholand^{1,2}, Dirk Voit⁴, Jens Frahm^{2,4}, and Martin Uecker^{1,2}¹Diagnostic and Interventional Radiology, University Medical Center Göttingen, Göttingen, Germany, ²German Center for Cardiovascular Research (DZHK), Göttingen, Germany, ³Cognitive Neurology, University Medical Center Göttingen, Göttingen, Germany, ⁴Biomedizinische NMR, Max-Planck-Institute for Biophysical Chemistry, Göttingen, Germany

Synopsis

To achieve dynamic and simultaneous access to R_2^* relaxation rates, B_0 field inhomogeneities and water/fat separation, we developed a model-based reconstruction technique on BART for continuous acquisitions based on undersampled multi-echo multi-spoke radial FLASH. Beside spatial smoothness constraints on coil sensitivity and B_0 field maps, L1 wavelet regularization is applied to the water, fat and R_2^* maps. Preliminary results of brain fMRI data demonstrate significant T_2^* change from 37 to 67 ms in the occipital visual cortex. In addition, R_2^* mapping of free-breathing liver with only 15 RF shots per frame (194 ms temporal resolution) reveals increased R_2^* during inspiration.

Introduction

Echo-planar imaging is an efficient acquisition scheme, capable of providing multi-contrast and multi-parametric images.¹ Moreover, multi-echo readout and radial sampling strategies emerge as a promising alternative to conventional breath-holding Cartesian sampling, e.g. for free-breathing quantitative R_2^* mapping of the liver.²⁻⁴ However, these techniques require moderate undersampling factors and hence physiological gating methods to overcome motion problems. In contrast, this work presents a model-based reconstruction technique for dynamic R_2^* and B_0 field inhomogeneity quantification in combination with simultaneous water/fat separation. Acquisitions are based on the multi-echo multi-spoke radial FLASH sequence, while first validating applications study the effects of brain activation and abdominal breathing on quantitative parameter maps.

Methods

The multi-echo multi-spoke radial FLASH sequence⁵ has been applied to dynamic water/fat separation⁶ based on triple-echo acquisition with asymmetric readouts⁷. Here, the echo train length (ETL) is elongated to allow for the inclusion of transversal magnetization relaxation (R_2^*) in the forward model,

$$F_{j,m}(x) = P_m \mathcal{F} \left\{ (W + F \cdot z_m) \cdot e^{-R_2^* TE_m} \cdot e^{i2\pi f_{B_0} TE_m} \cdot c_j \right\} \quad \text{with } x = (W, F, R_2^*, f_{B_0}, c_1, \dots, c_N)^T. \quad (1)$$

P_m and \mathcal{F} is the sampling pattern of the m th echo and 2D FFT, respectively. z_m is the six-peak fat spectrum at the m th echo time (TE_m). The unknown x contains the water (W), fat (F), R_2^* , and B_0 field inhomogeneity (f_{B_0}) maps as well as one set of coil sensitivity maps (c_j). The joint estimation of all unknowns in Equation (1) poses a non-linear non-convex inverse problem,

$$\Phi(\hat{x}) = \arg \min_{\hat{x}} \underbrace{\sum_{j=1}^N \sum_{m=1}^{\text{ETL}} \|y_{j,m} - F_{j,m}(T\hat{x})\|_2^2}_{\text{smooth}} + \alpha_n \|\hat{x} - \hat{x}_0\|_2^2 + \beta_n \|W(\hat{x} - \hat{x}_0)\|_1 \quad (2)$$

where a Sobolev-norm⁸ weight matrix (T) is applied onto f_{B_0} and c_j to enforce spatial smoothness. In addition, ℓ_1 wavelet joint sparsity constraint is applied onto the W, F and R_2^* maps. Given the non-smoothness of the ℓ_1 regularization term, IRGNM-FISTA⁹ is adapted to solve this problem. The derivative of the smooth part of Equation (2) supplies the normal equation for FISTA. This reconstruction technique has been implemented on BART¹⁰ and all reconstructions were run on TITAN Xp GPU (Nvidia, Santa Clara, CA, USA).

The initialization of the first frame is given by the estimated W, F and f_{B_0} using only the first three echoes, while both R_2^* and c_j are initialized with 0. The rationale is that this initialization strategy can better counteract potential phase wrapping from later echoes and foster convergence. The later frames are initialized by the estimate from their preceding frame, while \hat{x}_0 is set as the initialization damped by a factor of 0.9. The regularization strength is defined as $\alpha_n = \beta_n = (1/3)^{n-1}$ with the Newton iteration $n \in [1, 10]$.

Data acquisition were performed on a 3 T scanner (Magnetom Prisma, Siemens Healthineers, Erlangen, Germany) with a 64-channel head coil and an 18-channel body matrix coil for brain and liver studies, respectively. Details of the acquisition parameters are listed in Table 1. The brain functional MRI (fMRI) measurement lasted 258 seconds, and used a repetitive visual stimulation pattern (18-second black-and-white checkerboards) and control pattern (12-second gray field). In this preliminary study, a relatively low bandwidth and large echo spacing were used, so higher spatiotemporal resolution might be achieved with further optimization. The liver studies were conducted during free breathing without the use of gating methods.

Results

With radial sampling, as shown in Figure 1, the echo images with parallel imaging as nonlinear inverse reconstruction⁸ are resistant to spatial distortion artifacts. Moreover, the combined RSS image shows no visible signal loss caused by B_0 field inhomogeneity. Figure 2 shows the water, fat, R_2^* and f_{B_0} maps via the proposed model-based reconstruction and the time course of T_2^* values (i.e. $1000/R_2^*$) from three selected brain pixels. The T_2^* time course from the purple pixel within visual cortex shows significant change of T_2^* values, i.e. 27 ms increase from its baseline value 40 ms, corresponding to a relative change of 68%, while the other two pixels show only small noise-like T_2^* variations.

Figures 3 and 4 depict model-based reconstructions from multi-echo radial FLASH acquisitions with 33 and 15 shots per frame, respectively. No visible image degradation can be found for these degrees of undersampling. However, respiration motions perturb both B_0 field inhomogeneities (see the f_{B_0} maps in Figure 3) and R_2^* relaxation (time course of mean R_2^* in Figure 4), especially in the lower segment of liver and spleen. These changes most likely reflect the strong spin dephasing during organ movements when an air-tissue-like interface is created between lung and liver.

Discussion and Conclusion

Multi-echo radial sampling is well-suited for dynamic and quantitative imaging given its immunity to spatial distortion and resistance to motion. Moreover, dynamic R_2^* mapping via the proposed model-based reconstruction offers a direct measure of time-resolved R_2^* alterations in response to physiological changes.

Acknowledgements

No acknowledgement found.

References

1. Wang F, Dong Z, Reese TG, et al. Echo planar time-resolved imaging (EPTI). *Magn Reson Med*. 2019;81:3599-3615.
2. Armstrong T, Dregely I, Stemmer A, et al. Free-breathing liver fat quantification using a multiecho 3D stack-of-radial technique. *Magn Reson Med*. 2018;79:370-382.
3. Zhong X, Armstrong T, Nickel MD, et al. Effect of respiratory motion on free-breathing 3D stack-of-radial liver R_2^* relaxometry and improved quantification accuracy using self-gating. *Magn Reson Med*. 2019. doi: 10.1002/mrm.28052.
4. Schneider M, Benkert T, Solomon E, et al. Free-breathing water, fat, and iron quantification in the abdomen using radial multi-echo acquisition and respiratory-resolved model-based reconstruction. In Proceedings of the 27th Annual Meeting of ISMRM, Montreal, 2019. p. 1217.
5. Tan Z. Advances in real-time phase-contrast flow MRI and multi-echo radial FLASH. PhD thesis, University of Goettingen 2016.
6. Tan Z, Voit D, Kollmeier JM, et al. Dynamic water/fat separation and B_0 inhomogeneity mapping - Joint estimation using undersampled triple-echo multi-spoke radial FLASH. *Magn Reson Med*. 2019;82:1000-1011.
7. Untenberger M, Tan Z, Voit D, et al. Advances in real-time phase-contrast flow MRI using asymmetric radial gradient echoes. *Magn Reson Med*. 2016;75:1901-1908.
8. Uecker M, Hohage T, Block KT, et al. Image reconstruction by regularized nonlinear inversion - Joint estimation of coil sensitivities and image content. *Magn Reson Med*. 2008;60:674-682.
9. Wang X, Roeloffs V, Klosowski J, et al. Model-based T1 mapping with sparsity constraints using single-shot inversion-recovery radial FLASH. *Magn Reson Med*. 2018;79:730-740.
10. Uecker M, Ong F, Tamir JJ, et al. Berkeley advanced reconstruction toolbox (BART). In Proceedings of the 23rd Annual Meeting of ISMRM, Toronto, 2015. p. 2486.

Figures

	Brain		Liver	
Field of view (mm ²)	192 × 192		320 × 320	
Voxel size (mm ³)	1.5 × 1.5 × 4.0		1.0 × 1.0 × 6.0	
Flip angle (°)	16		8	
Bandwidth (Hz pixel ⁻¹)	510		1040	
Asymmetry	0.50		0.25	
Shots per frame	25		33	15
Echo train length	13		9	9
Repetition time (ms)	40		12.60	12.90
Acquisition time per frame (ms)	1000		416	194
Echo time (ms)	TE ₁ = 2.4	1.34, 2.86, 3.91	1.34, 2.92, 3.99	
	ESP = 3	5.43, 6.48, 8.00	5.57, 6.64, 8.22	
		9.05, 10.57, 11.62	9.29, 10.87, 11.94	

Table 1 Multi-echo multi-spoke radial FLASH acquisition parameters

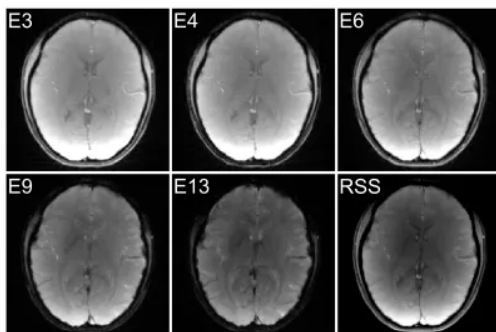


Figure 1 Multi echo images reconstructed via parallel imaging as nonlinear inversion (NLINV). Displayed images are the 3rd (TE of 8.4 ms), 4th (TE of 11.4 ms), 6th (TE of 17.4 ms), 9th (TE of 26.4 ms), and 13th (TE of 38.4 ms) echo, as well as the root of sum of squares (RSS) of all echoes

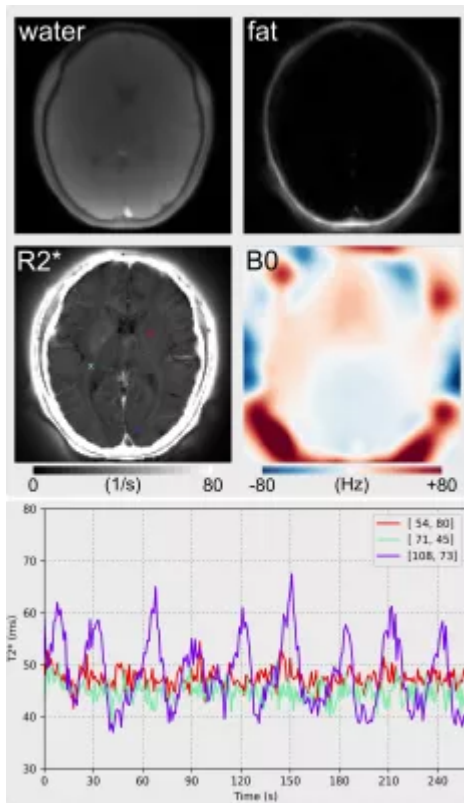


Figure 2 (Top) Water, fat, $R2^*$ and field inhomogeneity maps via the proposed multi-echo multi-spoke radial FLASH acquisition (25 shots per frame with an ETL of 13) and model-based reconstruction with 8 Newton iterations. (Bottom) The time course of $T2^*$ values from three selected pixels (colored cross marks in the $R2^*$ map). Significant visual cortex activation is observed from the pixel [108,73], whose $T2^*$ change is as large as 27 ms

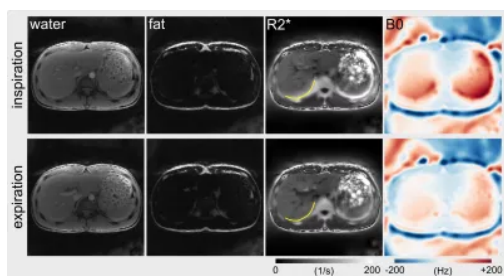


Figure 3 Model-based reconstructions of water, fat, $R2^*$ and field inhomogeneity maps from dynamic multi-echo multi-spoke radial FLASH acquisition (33 shots per frame with an ETL of 9). The top and bottom panels display the reconstruction results at the inspiration and respiration phase, respectively. The liver border (see the handcrafted yellow curve) indicates the breathing motion, resulting in increased $R2^*$ values

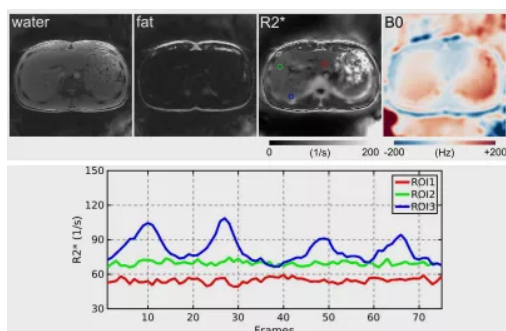


Figure 4 (Top) Model-based reconstructions of water, fat, $R2^*$ and field inhomogeneity maps from dynamic multi-echo multi-spoke radial FLASH acquisition (15 shots per frame with an ETL of 9) with a temporal resolution of 194 ms per frame. (Bottom) The time course of mean $R2^*$ values from three regions of interest (ROI). $R2^*$ values are changed due to breathing, especially in the third ROI